Structural Engineering and Mechanics, *Vol. 52, No. 5 (2014) 875-887*
DOI: http://dx.doi.org/10.12989/sem.2014.52.5.875

Shaking table experiment on a steel storage tank with multiple friction pendulum bearings

Ruifu Zhang*, Dagen Weng[a] and Qingzi Ge[b]

Research Institute of Structural Engineering and Disaster Reduction, Tongji University, 1239 Siping Road, Shanghai 200092, China

(Received March 26, 2013, Revised August 6, 2013, Accepted May 1, 2014)

Abstract. The aim of the shaking table experiment is to verify the isolation effect of a storage liquid tank with multiple friction pendulum bearings. A 1:20 scale model of a real storage liquid tank that is widely used in the petroleum industry was examined by the shaking table test to compare its anchored base and isolated base. The seismic response of the tank was assessed by employing the time history input. The base acceleration, wave height and tank wall stress were used to evaluate the isolation effect. Finally, the influences of the bearing performance that characterizes the isolated tank, such as the friction force and residual displacement, were discussed.

Keywords: tank; shaking table test; base isolation; multiple friction pendulum bearing; liquid solid coupling

1. Introduction

Tank damage occurs during earthquakes and introduces the need for seismic experiments and theoretical research on tanks. The seismic performance of a storage liquid tank is very complex, and the seismic performance of a storage tank was mainly observed experimentally in previous studies. Some aluminum tank models were tested by shaking the table to explore the gap between the seismic design method of tanks and the performance of actual tanks (Clough 1977). Shaking table experiments of three full-scale storage liquid tanks were performed by Haroun and Housner (1983) to verify the reliability of tank seismic theory and to improve the design method. In a traditional tank design, a tank is strengthened to resist seismic action, but the isolation design depends on additional elasticity and damping provided to decrease the seismic acceleration of the upward transmission.

There has been much focus on applying the isolation and energy dissipation system to storage liquid tanks. The traditional tank design method tends to use tanks with a low height-diameter ratio, but the isolation system may increase the height-diameter ratio (Tajirian 1998). An isolated tank and an anchored tank were compared by the shaking table test (Chalhoub and Kelly 1990),

*Corresponding author, Ph.D., E-mail: zhangruifu@gmail.com
[a]Professor, E-mail: wdg@tongji.edu.cn
[b]Ph.D. Student, E-mail: geqingzi@hotmail.com

http://www.techno-press.org/?journal=sem&subpage=8 ISSN: 1225-4568 (Print), 1598-6217 (Online)

which verified the advantageous effect of the isolated tank and showed the reliability of elasto-plastic bearings for reducing the seismic response. In a shaking table experiment of a 1:14 steel tank with sliding bearings and high-damping rubber isolators, the seismic response of the isolated storage liquid tank was investigated (De Angelis *et al.* 2009, Paolacci *et al.* 2009). A storage tank may have a low temperature or contain corrosive substances, and the liquid level of the tank during normal operation is constantly changing, which significantly influences the isolated system's vibration period. Thus, rubber type bearings are not recommended for the seismic isolation of storage tanks. Recent studies focus on friction pendulum bearings (FPBs), mainly because the fundamental period of tanks isolated by an FPB merely depends on the radius of curvature of the sliding interface, making the dynamic characteristics of the isolated tanks invariant and fully controllable, regardless of the storage level. Made of stainless steel, an FPB is also resistant to chemicals, fires, temperature extremes, and adverse environmental exposure. Given the above advantages, an FPB can ensure effective and durable isolation for industrial tank applications (Wang *et al.* 2001). The efficiency of an FPB system for an isolated tank is investigated by parametric analysis (Abali and Uckan 2010), but the diameter of an FPB is too large, especially when used in soft sites. A multiple friction pendulum bearing (MFPB), which has a large diameter and improves on the FPB, was studied widely (Fenz and Constantinou 2008, Morgan and Mahin 2011, Soni *et al.* 2011, Tsai and Lin 2011), and an MFPB is better for the structure because of its long substantial period and large isolation story displacement. The effectiveness of an isolated steel storage tank with MFPBs was investigated through numerical models (Zhang *et al.* 2011), but an isolated storage liquid tank with MFPBs needs to be checked experimentally. Previous work on a rigid wall tank with an MFPB was conducted by Calugaru and Mahin (2009). In this experiment, the whole liquid was isolated because of the large scale. However, in many actual cases, it is difficult to isolate the convective component, and only the impulsive component of the liquid can be isolated.

In this paper, a shaking table experiment was conducted on a reduced-scale model in both anchored and isolated tanks using MFPBs. Dynamic system identification was carried out to evaluate the modal properties. The seismic response of the tank was assessed by employing the time history input. The seismic response quantities, including the acceleration, tank wall stress, isolation layer displacement and wave height, were discussed and compared between the anchored and isolated tanks.

2. Vibration control device

A friction isolation system includes an FPB, which has two properties, the friction sliding effect and a restoring force produced by geometric shapes (Al-Hussaini *et al.* 1994). The double concave friction pendulum (DCFP) system (Fig. 1) improves on the single concave friction pendulum system (SCFP). The slider and the spherical concave surface utilize coating with a low friction coefficient. The restoring force of the bearing system is provided by the slider, which may move in the concave surface and cause mass uplift. Some damping and the effectiveness stiffness of the isolation bearing are provided by the slider and concave surface, and the concave radius of the bearing determines the isolation period. An MFPB has a larger concave radius and friction coefficient, which brings more flexibility for an isolation design (Tsai *et al.* 2003).

The DCFP can be understood as combination of two SCFPs (Constantinou *et al.* 1999). The isolation period T of a DCFP can be expressed as

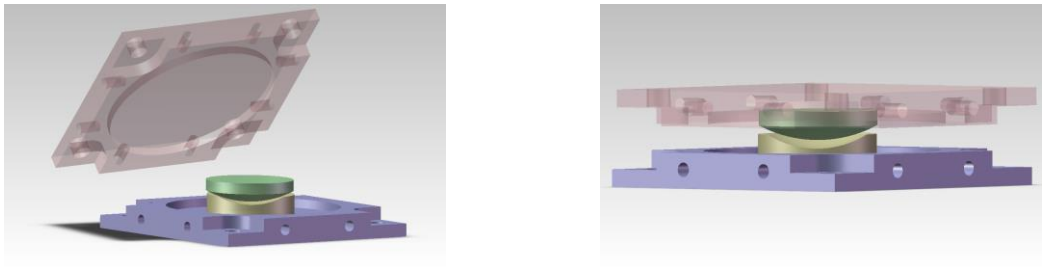

(a) (b)

Fig. 1 DCFP system

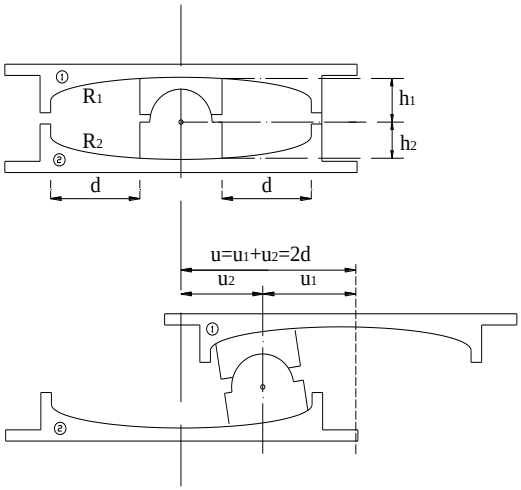

Fig. 2 Cross section of the DCFP bearing

$$T = \sqrt{T_1^2 + T_2^2} = 2\pi\sqrt{\frac{R_1 + R_2}{g}} \tag{1}$$

where the subscripts 1 and 2 refer to the upper and lower concave surfaces, respectively. R is the concave surface radius, and g is the gravitational acceleration.

The force-displacement relationship of the DCFP can be expressed as

$$\begin{aligned} F &= F_r + F_f \\ &= \frac{W}{R_1 + R_2}u + \frac{R_1\mu W\,\mathrm{sgn}(\dot{u}_1) + R_2\mu W\,\mathrm{sgn}(\dot{u}_2)}{R_1 + R_2} \\ &= K_b u + F_f \end{aligned} \tag{2}$$

$$\mu = \mu_{\max} - (\mu_{\max} - \mu_{\min})\exp(-\alpha|\dot{u}|) \tag{3}$$

where F is the horizontal force, F_r is the restoring force of the sliding surface, F_f is the friction force of the sliding surface, W is the vertical load, u is the relative displacement of the slider between the upper and lower concave surfaces, α is a control parameter and the inverse of velocity,

Fig. 3 Liquid level

Fig. 4 Tank model

μ is used to describe the DCFP friction coefficient, and the subscripts max and min mean a large velocity and a nearly zero sliding velocity, respectively. A cross sectional schematic diagram of a DCFP bearing is shown in Fig. 2. 2*d* is the maximum sliding displacement of the DCFP bearing.

For an FPB system, if the relative displacement is smaller than a certain value in Eq. (4),the restoring force is smaller than the friction force, and the bearing will not recenter (Naeim and Kelly 1999).

$$u / R \le \mu \tag{4}$$

3. Shaking table tests

The experiment was carried out using the 4×4 m shaking table installed in the State Key Laboratory for Disaster Reduction in the Department of Civil Engineering, Tongji University, China.

3.1 Scaling factor

Storage liquid tanks are used in chemistry, petrochemistry and other industries and are an important piece of equipment. The prototype tank has a diameter of D=80 m, a liquid level of H=24 m, a liquid density of ρ=480 kg/m^3 and a wall thickness between 10 and 20 mm.

The full-scale experiment cannot be conducted on the shaking table for most storage liquid tanks because of their large size, and the option of key parameters is important for the scaled tank model. Eq. (5) may be used to describe the vibration of the storage liquid tank (Haroun and Housner 1983)

$$\left.\begin{aligned} T_c &= 1.8\frac{0.578}{\sqrt{\tanh(\frac{3.68H}{D})}}\sqrt{D} \\ T_i &= (\frac{1}{\sqrt{2000}})(\frac{C_i H}{\sqrt{\frac{t_u}{D}}})(\frac{\sqrt{\rho}}{\sqrt{E}}) \end{aligned}\right\} \tag{5}$$

where T_c is the convective period, T_i is the impulsive period, D is the diameter, H is the liquid level, C_i is a non-dimensional coefficient, t_u is the wall thickness, ρ is the liquid density and E is the wall's elastic modulus. Eq. (5) indicates that T_c is proportional to D. However, T_i is not only affected by D and is also related to t, ρ and E. Theoretically, the dynamic equivalence between the scaled and full-scale tanks can be found. However, the commonly used materials have some limitations. For example, a very thin tank wall may lead to tank instability and failure to bear the weight of the liquid. Thus, it is impossible to obtain the appropriate scale factor between the scaled and full-scale tanks if only using geometric scaling (De Angelis *et al.* 2009). The difference between the convective period and impulsive period is too large based on the above consideration, so only the main parameters can be selected in the model design. Eq. (5) may be expressed as

$$\left.\begin{aligned} S_{T_c} &= \sqrt{S_L} \\ S_{T_i} &= \sqrt{S_L^3 S_{\rho_f} / \left(S_{t_s} S_{E_s}\right)} \end{aligned}\right\} \tag{6}$$

The scale relationship and the meanings of the scale parameters are shown in Table 1.

Thus, the geometric scale factor is approximately 20. Because the period of the convective mode is a function of the squared dimensions, the time scale of the convective motion is 4.47. To obtain the same scale ratio for the impulsive period, the thickness should be reduced to 1/192 of the real one. This is obviously impossible, and only one time scale can be respected (De Angelis *et al.* 2009). The model's period is less than that of the prototype tank, which means that the input of the time history wave should be compacted. However, the scale factors are very different between the convective period and the impulsive period, and the shaking table's excitation frequency is limited. If the frequency of the original seismic wave is compacted according to the impulsive

Table 1 Scale relationship and scale factors

Parameter		Scale relationship	Scale factor (prototype/model)
Geometry	L	S_L	20
Convective period	T_c	$S_{T_c} = \sqrt{S_L}$	4.47
Elastic modulus	E_s	S_{E_s}	1
Fluid density	ρ_f	S_{ρ_f}	0.48
Wall thickness	t_s	S_{t_s}	14
Impulsive period	T_i	$S_{T_i} = \sqrt{S_L^3 S_{\rho_f} / \left(S_{t_s} S_{E_s}\right)}$	16.56
Time	t	S_t	16.56
Acceleration	a	$S_a = S_L / S_t^2$	0.073
Impulsive frequency	f	$S_f = 1/S_{T_i}$	0.06
Impulsive mass	m_i	$S_{m_i} = S_L^3$	8000
Gravity acceleration	g	S_g	1
Impulsive height	h_i	$S_{h_i} = S_L$	20
Wave height	h_w	$S_{h_w} = S_L S_a / S_g$	1.46

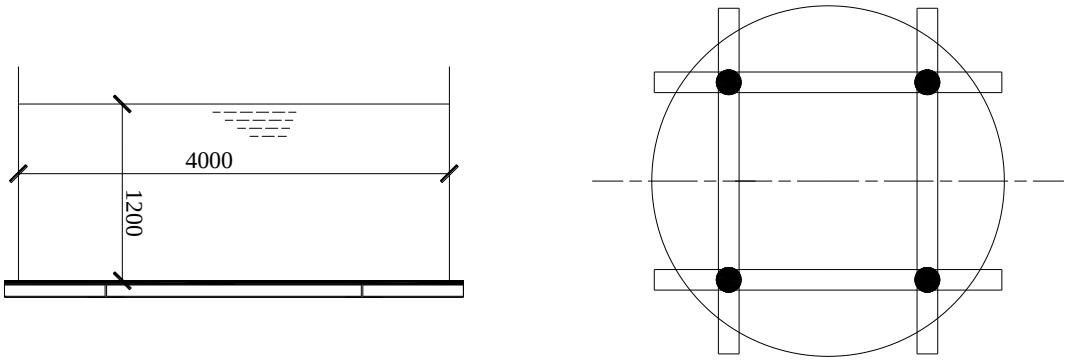

(a) (b)

Fig. 5 Plan and section schematic diagrams of the tank model

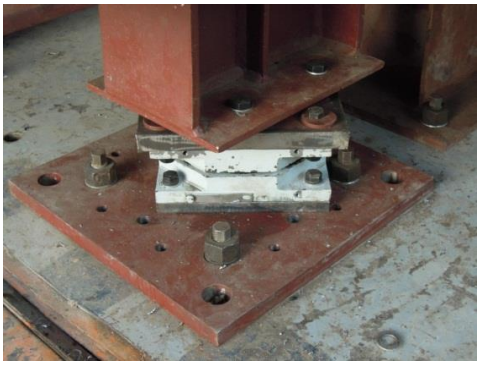

Fig. 6 DCFP under the model tank

scale, signal distortion of the shaking table input can occur. Therefore, it is impossible to compact the seismic wave according to the scale factor of the impulsive or convective periods. The main purpose of this experiment is to use MFPBs to produce the isolation effect of impulsive mass. The impulsive frequency of the model tank is still located in the high frequency band of the original seismic wave spectrum, and the original non-compacted waves are used in the test. The model's isolation bearing should be selected with a period $\sqrt{2}$ times greater than the model's impulsive period.

3.2 Tank model design

The scaled model has a diameter of D_m=4 m, a liquid height of H_m=1.2 m and a wall thickness of t_s=1.5 mm. A steel plate and H-shaped steel beams are used under the tank.

3.3 Base isolation systems design

The manufacturer provides the appropriate bearing according to the requirement of the experimental design parameters. Moreover, a preparative test is performed before the formal test to acquire the actual parameters. In the preparative test, bearing force transducers are used. The

Table 2 Parameters of the DCFP

Bearing capacity	μ_{min}	μ_{max}	R_1	R_2	T	D_p
ton			m	m	s	mm
7	0.04	0.13	1.1	1.1	3.0	150

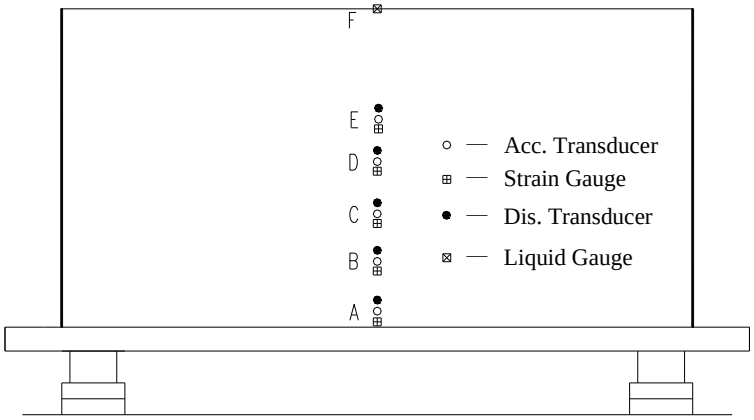

Fig. 7 Schematic diagram of the main sensors placment

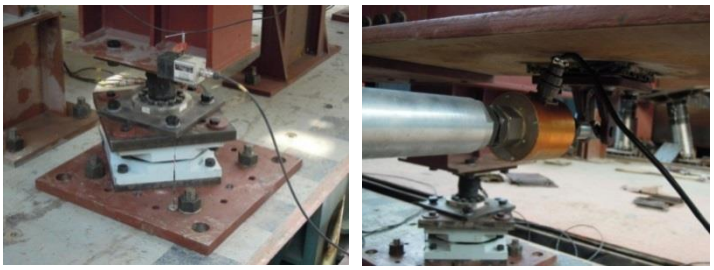

Fig. 8 Schematic diagram of the main sensors

bearing parameters are shown in Table 2, and D_p is the designed maximum displacement.

3.4 Test set-up

Sensors, which include a liquid gauge, acceleration transducers, displacement transducers and strain gauges, were used to measure the dynamic response of the tank model (Fig. 7). The tank's acceleration and displacement were measured by acceleration and displacement transducers, respectively. The liquid gauge was used for the liquid sloshing motion, and a strain gauge was used for the tank wall strain. The table's motion was monitored by several accelerometers. In the isolation layer, the bearing motions were measured by force and displacement transducers (Fig. 8).

3.5 Seismic wave selection

Six natural waves were used in the shaking table experiment according to the Chinese Code Spectrum (Site Ⅲ), and the peak value could be scaled. The natural records were selected from

Table 3 Characteristics of the natural waves

NGA	Accelerogram	Year	Station	Epicenter distance (km)	Magnitude
779	Loma Prieta	1989	LGPC	0	6.93
1084	Northridge-01	1994	Sylmar-Converter Sta	0	6.69
1504	Chi-Chi-Taiwan	1999	TCU067	0.6	7.62
1605	Duzce- Turkey	1999	Duzce	0	7.14
1158	Kocaeli-Turkey	1999	Duzce	13.6	7.51
776	Loma Prieta	1989	Hollister-South & Pine	27.7	6.93

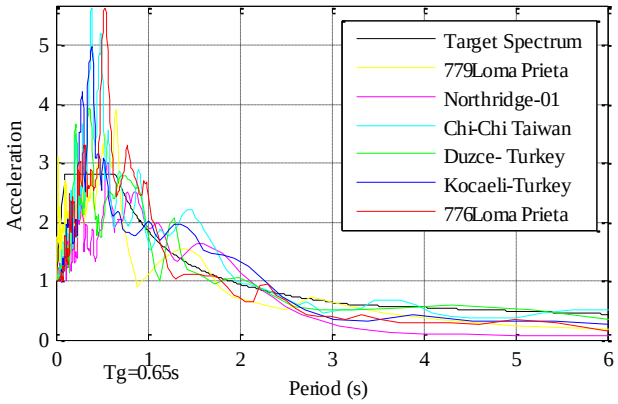

Fig. 9 Normalized response spectrum curves

the Pacific Earthquake Engineering Research Center database and were used to obtain the structure's dynamic responses. The natural waves used in the experiment are described in Table 3, and the target spectrum and the spectra of all waves are shown in Fig. 9.

4. Results analysis

4.1 Identification of the dynamic characteristics

At the beginning of experimental, the tank's convective and impulsive frequencies were identified. For both the anchored tank and the isolated tank under different ground motions, the wave height time histories of the free liquid surface were converted by a Fourier transform into spectra, which were used to obtain the convective frequencies of the tank model. The impulsive frequencies were determined by the transfer functions between the tank's input and output signals. For the anchored tank model, the experimental impulsive frequency (36.74 Hz) was significantly different from the convective frequency (0.45 Hz). A numerical model was also built to compare the fundamental period with that of the test model. Four-noded, 24-DOF quadrilateral elastic shell elements (SHELL 63) that have both membrane and bending capabilities were used to model the walls of the tank. The fluid domain was modeled with three-dimensional eight-noded, 24-DOF fluid (solid) elements (FLUID 80). These elements had 3 DOF at each node (displacement in three directions). The interaction between the tank and the fluid was addressed by properly coupling the

Table 4 Frequency of anchored modal storage liquid tank (Hz)

	Numerical Method (model)	Experimental Method (model)	Numerical Method (prototype)
Convection	0.41	0.45	0.09
Impulsion	39.92	36.74	2.43

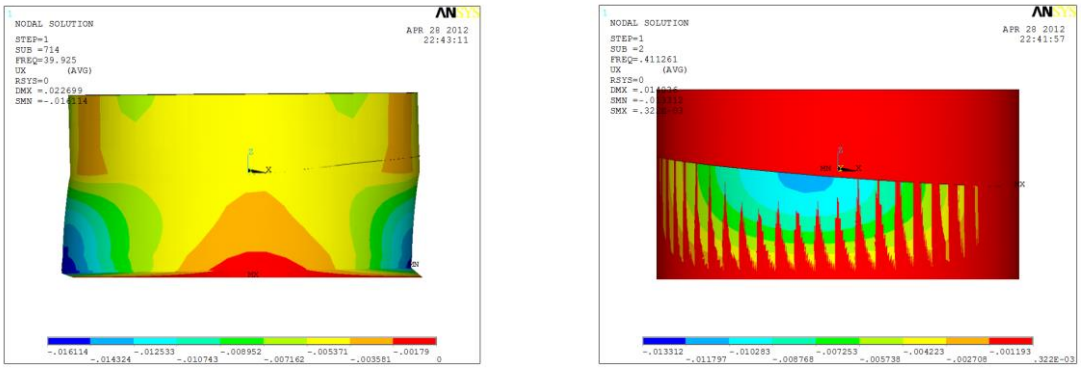

(a) (b)

Fig. 10 Modal tank model: (a) impulsive model; (b) convective model

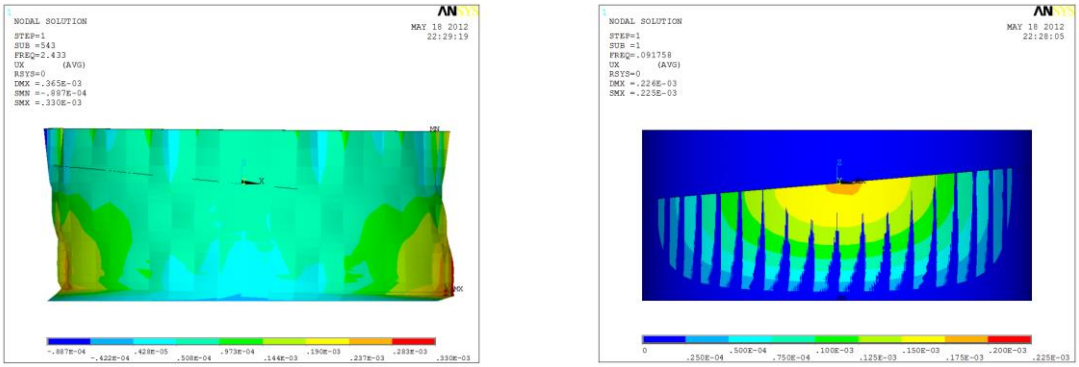

(a) (b)

Fig. 11 Prototype tank model: (a) impulsive model; (b) convective model

nodes that lie in the common faces of these two domains in the radial direction; the fluid cannot separate from the tank wall but can move in a transverse direction and can apply only normal pressures on the tank wall. The experimental and numerical frequencies of the anchored tank model are compared in Table 4, and the experimental convective frequency (0.45 Hz) was similar to the numerical convective frequency. In comparison with the anchored model tank, the isolated tank model's impulsive frequency (approximately 0.1 Hz) was significantly changed, but its convective motion was not changed by the isolation method. The modes of the numerical modal tank and the prototype tank are shown in Fig. 10 and Fig. 11, respectively.

The anchored and isolated schemes were conducted as follows:

ST1: anchored model tank.

ST2: isolated model tank.

Table 5 Peak values

Case	Response	NGA					
		779	1084	1504	1605	1158	776
ST1	Peak table acceleration (g)	0.41	0.29	0.32	0.41	0.34	0.33
	Peak table displacement (mm)	14	28	17	7	9	26
	Peak water elevation at the tank wall (mm)	233	224	168	181	191	226
ST2	Peak base acceleration (g)	0.11	0.11	0.15	0.12	0.12	0.11
	Peak base absolute displacement (mm)	46	47	58	45	39	36
	Peak water elevation at the tank wall (mm)	228	202	181	190	195	228

4.2 Response of the base-isolated tank

The dynamic responses of a cylindrical storage liquid tank anchored or isolated on the shaking table were compared in the present study. The tank wall's acceleration, wave height, isolation layer displacement and tank wall stress were used to evaluate the tank's seismic response. Because of the tank model's size, the tank wall's deformations were not studied and measured in detail.

The pressure on the tank wall is greatly dependent on the acceleration of the tank base (Chalhoub and Kelly 1990). In general, the input acceleration in the response was more apparent from the anchored tank than from the isolation tank, and the isolation system can greatly change the tank base's acceleration. The base acceleration and tank bottom's displacement can be found from the peak table acceleration and displacement of the shaking table for the anchored tank model. The peak base acceleration and absolute displacement can be measured by sensors. The peak liquid elevation is also important for both the anchored and isolated tank models. These dynamic responses of the tank model are shown in Table 5.

In the test, the tank was loaded by a stepwise loading method. When the peak acceleration value of the seismic wave was small (e.g., 0.1 g), the DCFPs could not slide and had no isolation effect because the seismic action could not produce a force larger than the maximum static friction force. For different horizontal seismic waves, the average peak table acceleration was 0.35 g. Table 5 shows that the peak base accelerations for the isolated model tank decreased by approximately 65% compared with the peak table accelerations for the anchored model tank. This result shows that the peak base acceleration can be decreased dramatically by the DCFP isolation system.

The frequency and acceleration of the shaking table are relatively high compared to the convective frequency of the model tank. Thus, the values cannot provide great responses of the convective component of the model tank. The ST2-to-ST1 ratio of the peak water elevation is approximately 1.01. The peak water elevations of the isolated model tank are slightly larger than those of the anchored model tank. Fig. 12 shows a displacement time history of the water free surface.

The mean of the peak table displacement is approximately 17 mm, and the mean of the absolute peak base displacement is approximately 45 mm. The isolation effect of the tank is obtained using DCFPs. Furthermore, the bearings have some energy dissipation capacity, and the hysteretic hoop is shown in Fig. 14. However, at the end of seismic action, the bearings have a residual displacement (Fig. 13) because the restoring force of the bearings is smaller than the friction force. Actual industry tanks have many pipe connections and equipment. The residual displacement can

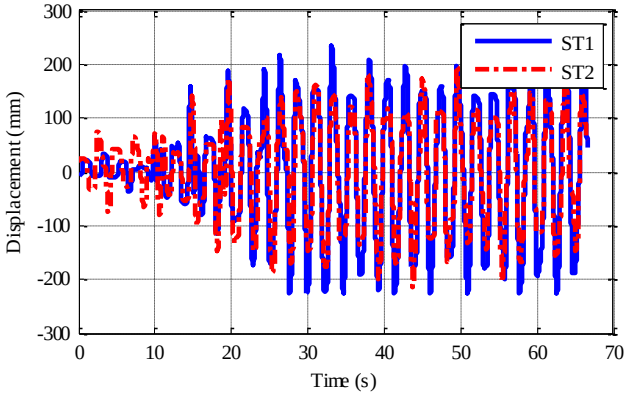

Fig. 12 Wave height's time history

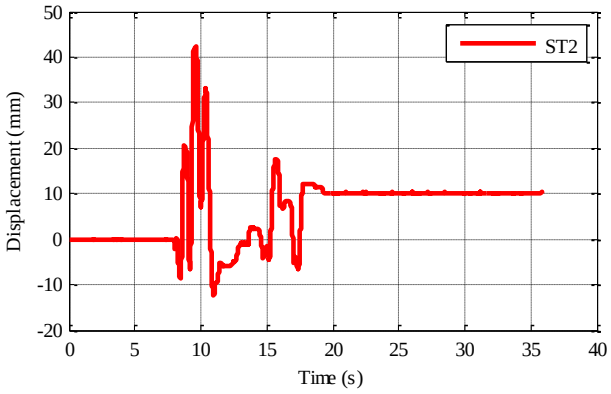

Fig. 13 Bearing displacement

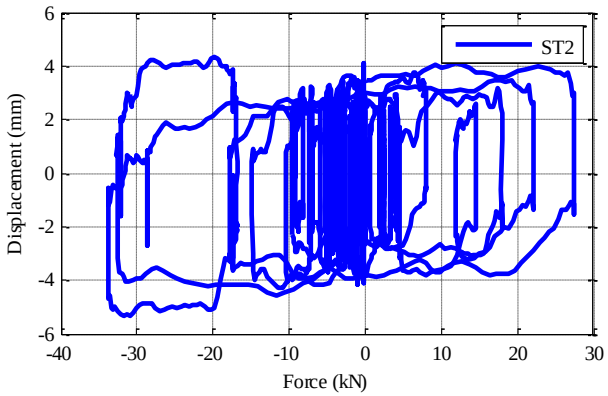

Fig. 14 Hysteretic hoop

make the operation recovery of a tank with pipe connections and the installation of equipment quite difficult after an earthquake. This is unfavorable for the post-earthquake normal operation of the storage tank.

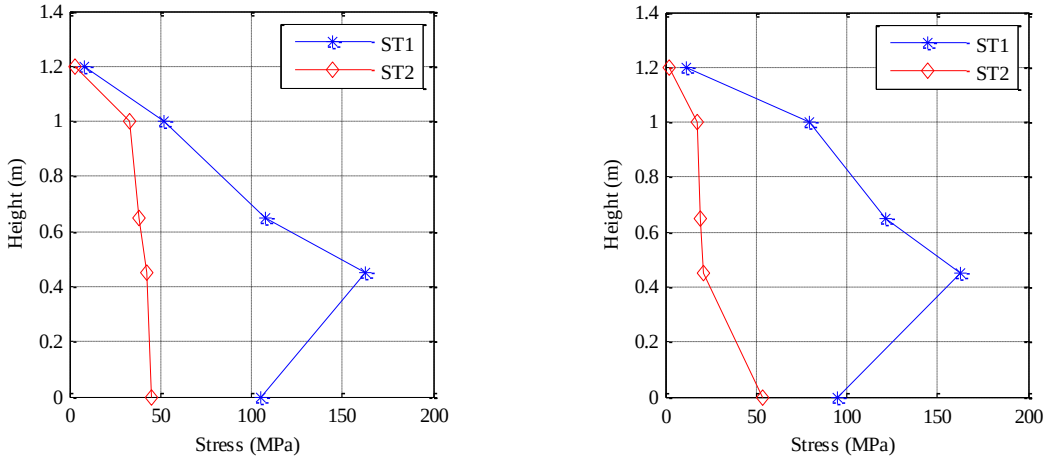

(a) (b)

Fig. 15 Tank wall stress: (a) circle stress; (b) axis stress

From a structural perspective, it is necessary to study the tank wall's stresses, especially the influence of the isolation system. The averages of the circular and axial tank wall stresses were measured at different locations (Fig. 15). The stress interpolations along the height direction were used in Fig. 15. The figure shows that the tank wall's weak positions were improved and the overall stresses were reduced. However, limited by the experimental condition, no pressure transducers were used in the experiment. The base shear coming from the convective and the impulsive pressure were not evaluated.

5. Conclusions

The seismic response of a storage liquid tank greatly depends on the form of support. A storage liquid tank (1:20) with anchored and isolated bases was examined by the shaking table test. Base isolation by MFPBs may drastically reduce the amplification of seismic accelerations for the base acceleration in the isolation case. The tank wall's stress may be decreased by the low frequency characteristics of the base isolated tank, and the weak location of the tank wall may be improved. The isolation period and friction force are affected by the vertical weight, but only the impulsive component may be isolated by MFPBs. Base isolation with MFPBs is very favorable for the storage liquid tank as a whole, but it cannot take effect in a low intensity earthquake and may bring some residual displacement of the bearings. The wave height changes are not obvious for different base forms, so it is difficult to decrease the response of the convective component, especially for large tanks.

Acknowledgments

This work was supported by the National Natural Science Foundation of China under Grant No. 51308418 and 51178355.

References

Abali, E. and Uckan, E. (2010), "Parametric analysis of liquid storage tanks base isolated by curved surface sliding bearings", *Soil Dyn. Earthq. Eng*., **30**(1-2), 21-31.

Al-Hussaini, T.M., Zayas, V.A. and Constantinou, M.C. (1994), "Seismic isolation of multi-story frame structures using spherical sliding isolation systems", National Center for Earthquake Engineering Research, State University of New York at Buffalo.

Calugaru, V. and Mahin, S.A. (2009), "Experimental and analytical studies of fixed base and seismically isolated liquid storage tanks", San Francisco, USA

Chalhoub, M.S. and Kelly, J.M. (1990), "Shake table test of cylindrical water tanks in base-isolated structures", *J. Eng. Mech*., **116**(7), 1451-1472.

Clough, D.P. (1977), "Experimental evaluation of seismic design methods for broad cylindrical tanks", Earthquake Engineering Research Center, University of California, Berkeley.

Constantinou, M.C., Tsopelas, P., Kasalaniti, A. and Wolff, E.D. (1999), "Property modification factors for seismic isolation bearings", Multidisciplinary Center for Earthquake Engineering Research, State University of New York at Buffalo, Buffalo, NY, USA.

De Angelis, M., Giannini, R. and Paolacci, F. (2009), "Experimental investigation on the seismic response of a steel liquid storage tank equipped with floating roof by shaking table tests", *Earthq. Eng. Struct. Dyn*., **39**(4), 377-396.

Fenz, D.M. and Constantinou, M.C. (2008), "Spherical sliding isolation bearings with adaptive behavior: Experimental verification", *Earthq. Eng. Struct. Dyn*.,**37**(2), 185-205.

Haroun, M.A. and Housner, G.W. (1983), "Vibration studies and tests of liquid storage tanks", *Earthq. Eng. Struct. Dyn.*,**11**(2), 179-206.

Morgan, T.A. and Mahin, S.A. (2011), "The use of base isolation systems to achieve complex seismic performance objectives", Pacific Earthquake Engineering Research Center, University of California, Berkeley.

Naeim, F. and Kelly, J.M. (1999), *Design of seismic isolated structures: From theory to practice*, John Wiley & Sons, Inc., Canada.

Paolacci, F., Giannini, R. and de Angelis, M. (2009), "Experimental investigation on the seismic behaviour of a base-isolated steel storage tank", *11th World Conference on Seismic Proceedings of Isolation, Energy Dissipation and Active Vibration Control of Structures*, Guangzhou, China.

Soni, D.P., Mistry, B.B. and Panchal, V.R. (2011), "Double variable frequency pendulum isolator for seismic isolation of liquid storage tanks", *Nucl. Eng. Des*., **241**(3), 700-713.

Tajirian, F.F. (1998), "Base isolation design for civil components and civil structures", *Proceedings of Structural Engineers World Congress, San Francisco*, California, USA

Tsai, C.S., Chiang, T.C. and Chen, B.J. (2003), "Seismic behavior of MFPS isolated structure under near-fault sources and strong ground motions with long predominant periods", *Seismic Eng*., **466**, 73-79.

Tsai, C.S. and Lin, Y.C. (2011), "Characterization and shaking table tests of multiple trench friction pendulum system with numerous intermediate sliding plates", *Struct. Eng. Mech*., **40**(2), 167-190.

Wang, Y.P., Teng, M.C. and Chung, K.W. (2001), "Seismic isolation of rigid cylindrical tanks using friction pendulum bearings", *Earthq. Eng. Struct. Dyn.*, **30**(7), 1083-1099.

Zhang, R.F., Weng, D.G. and Ren, X.S. (2011), "Seismic analysis of a LNG storage tank isolated by a multiple friction pendulum system", *Earthq. Eng. Eng. Vib.*, **10**(2), 253-262.